

# Influence of extreme events on sedimentation in sedimentation fields enclosed by brushwood fences

A. Matheja

*Franzius-Institute for Hydraulic, Waterways and Coastal Engineering, University of Hannover, Germany*

O. Stoschek

*Franzius-Institute for Hydraulic, Waterways and Coastal Engineering, University Hannover, Germany*

**ABSTRACT:** To ensure the safety of coastal defense systems along the German Wadden Sea coast, sedimentation fields were used for many centuries as sedimentation traps to increase natural sedimentation, speed up foreland growth and thus realize sustainable foreland development. To analyze sedimentation and erosion processes, two test sections have been surveyed. Selected field data and additional data from laboratory experiments were used for parameter identification. Comparison of model results with field recordings in the test area „Ockholm“ was used as a quality criterion for the applicability and efficiency of the employed numerical methodology. A numerical parameter study on the influence of currents, induced by tide and waves under mean long-term conditions, on sediment transport and thus sedimentation and erosion processes was performed. A second parameter study on the influence of extreme events was realized, which is comparing with systems behavior under mean conditions.

## 1 INTRODUCTION

At the German North Sea Coast forelands and salt marshes in front of sea dikes contribute significantly to protection and safety of the artificial coastline. In this way forelands are an important element of coastal protection systems.

Salt marshes and fore lying mud flats are formed by deposition of fine silts and sands in sheltered locations and colonized by specialized salt tolerant plants.

Sea level rise and increased frequency and intensity of storm tides may endanger forelands resulting in losses of sediment or reduction thereby decreasing wave attenuation and thus increasing erosion.

Within a research program on the optimization of foreland management, field measurements in sedimentation fields, physical experiments, and numerical simulations have been carried out to analyze the interaction of waves, currents, sedimentation processed, maintenance technique and field design.

Numerical parameter studies highlighted the effects of system geometry, dimensions of the drainage system, construction of fences and permeability of the system in relation to boundary conditions (tides and wave heights) on mud transport, sand transport and hence on sedimentation and erosion.

## 2 METHODOLOGY

### 2.1 Basic Approach

To analyze sedimentation and erosion processes (i.e. velocities, sedimentation rates and distribution) from the approaching sea and inside the fields (Fig. 1) under varying conditions, two local areas have been surveyed over a period of three years.

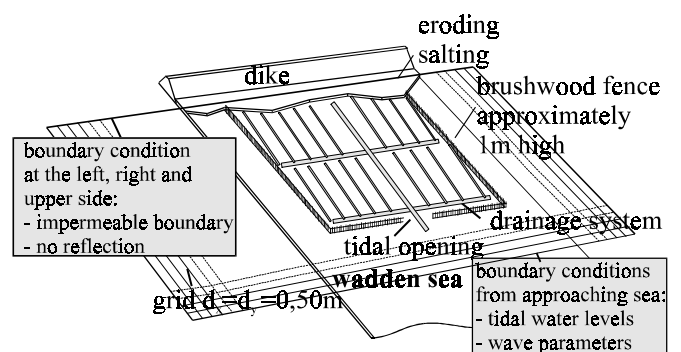


Figure 1. Sedimentation fields enclosed by brushwood fences used in the German Wadden Sea.

Selected data from these areas and data from physical experiments was used for parameter identification (friction parameter to simulate permeability of brushwood fences) and to calibrate a two-dimension-

nal numerical hydrodynamic model (MIKE21 HD-module), including a wave model (EMS-module) and a sediment transport model (MT-module). Comparison with field recordings in the test area „Ockholm“ was used as a quality criterion for the applicability and efficiency of the employed numerical methodology (Matheja et al. 1997). Numerical problems with the applied simulation system MIKE21 indicated, that the implemented numerical methods have limitations in extreme shallow tidal waters. These limitations result from system parameters (minimal slope of bathymetry, permeable behavior of brushwood fences, geometric description of drainage system) and from implementation characteristics of the applied numerical models (treatment of dried and flooded cells - chain problems and stability of the solver). However, these limitations have been overcome and results show satisfactory agreement.

A numerical parameter study on the influence of currents, induced by tide and waves under mean long-term conditions, on sediment transport and thus sedimentation and erosion processes was performed. Simulations showed the effects of system geometry, dimension of the drainage system (ditches), construction of fences and permeability of the system (earth embankment). It could also be shown, that averaged input parameters (mean tide, characteristic wave heights and sediment characteristics under these conditions) are not always sufficient to describe overall system behavior.

So a second parameter study for extreme events was realized. It showed the effects of rising water levels, changing wave heights and varying sedimentation input (fractions and concentrations).

## 2.2 Numerical simulation

### 2.2.1 Hydrodynamic module

The following equations, the conservation of mass and momentum integrated over the vertical, describe the flow and water level variations:

$$\frac{\partial \zeta}{\partial t} + \frac{\partial p}{\partial x} + \frac{\partial p}{\partial y} = 0 \quad (1)$$

$$\begin{aligned} & \frac{\partial p}{\partial t} + \frac{\partial}{\partial x} \cdot \left( \frac{p^2}{h} \right) + \frac{\partial}{\partial y} \cdot \left( \frac{p \cdot q}{h} \right) + g \cdot h \cdot \frac{\partial \zeta}{\partial x} \\ & + \frac{g \cdot p \cdot \sqrt{p^2 + q^2}}{C^2 \cdot h^2} - \frac{1}{\rho_w} \cdot \left[ \frac{\partial}{\partial x} \cdot (h \cdot \tau_{xx}) + \frac{\partial}{\partial y} \cdot (h \cdot \tau_{xy}) \right] \quad (2) \\ & - \Omega \cdot q - c_d \cdot V \cdot V_x + \frac{h}{\rho_w} \cdot \frac{\partial p_a}{\partial x} = 0 \end{aligned}$$

$$\begin{aligned} & \frac{\partial q}{\partial t} + \frac{\partial}{\partial y} \cdot \left( \frac{q^2}{h} \right) + \frac{\partial}{\partial x} \cdot \left( \frac{p \cdot q}{h} \right) + g \cdot h \cdot \frac{\partial \zeta}{\partial y} \\ & + \frac{g \cdot q \cdot \sqrt{p^2 + q^2}}{C^2 \cdot h^2} - \frac{1}{\rho_w} \cdot \left[ \frac{\partial}{\partial y} \cdot (h \cdot \tau_{yy}) + \frac{\partial}{\partial x} \cdot (h \cdot \tau_{xy}) \right] \quad (3) \\ & - \Omega \cdot p - c_d \cdot V \cdot V_y + \frac{h}{\rho_w} \cdot \frac{\partial p_a}{\partial y} = 0 \end{aligned}$$

where:

$h(x,y,t)$	water depth [m]
$\zeta(x,y,t)$	surface elevation [m]
$p, q(x,y,t)$	flux density in x-/y-direction [ $m^3/s/m$ ]
$C(x,y)$	Chezy resistance [ $m^{0.5}/s$ ]
$f(V)$	wind friction factor [-]
$V, V_x, V_y(x,y,t)$	wind speed in x-/y-direction [m/s]
$\Omega(x,y)$	Coriolis parameter [ $s^{-1}$ ]
$p_a(x,y,t)$	atmospheric pressure [ $kg/m/s^2$ ]
$\rho_w$	density of water [ $kg/m^3$ ]
$x,y$	coordinates [m]
$t$	time [s]
$\tau_{xx}\tau_{xy}\tau_{yy}$	effective shear stresses [ $N/m^2$ ]

The implemented algorithm makes use of the ADI algorithm („Alternating Direction Implicit“) to integrate the equations in the space-time domain. The difference terms are expressed on a staggered grid and solved by the double sweep algorithm (Richtmeyer & Morton 1967).

### 2.2.2 Elliptic mild-slope wave model

The basic equation is the „mild-slope“ equation (Berkhoff 1972) for time-harmonic problems:

$$\nabla (C_g C \nabla \xi) = \frac{C_g}{C} \frac{\partial \xi}{\partial t^2} \quad (4)$$

where:

$C_g$	group celerity [m/s]
$C$	wave celerity [m/s]
$\xi$	surface elevation [m]

By introducing pseudo fluxes and generalizing the equations to include wave generation, sponge layer absorption, partial reflection, bed friction and wave breaking, this equation can be rewritten as a system of first order equations (Warren et al. 1985 and Madsen & Larsen 1987), which leads to:

$$\frac{C_g}{C} \frac{\partial S}{\partial t} + \left( \frac{C_g}{C} i\omega + f_s \right) S + \frac{\partial P}{\partial x} + \frac{\partial Q}{\partial y} = SS \quad (4)$$

$$\begin{aligned} & \frac{C_g}{C} \frac{\partial P}{\partial t} + \left( \frac{C_g}{C} \omega(i + f_p) + f_s + e_f + e_b \right) P \\ & + C_g^2 \frac{\partial S}{\partial x} = 0 \end{aligned} \quad (5)$$

$$\frac{C_g}{C} \frac{\partial Q}{\partial t} + \left( \frac{C_g}{C} \omega(i + f_p) + f_s + e_f + e_b \right) Q + C_g^2 \frac{\partial S}{\partial y} = 0 \quad (6)$$

- where  
*S, P, Q* complex functions of x, y and t  
 $\omega$  wave frequency [1/s]  
*i* imaginary unit  
*SS* source magnitude per unit horizontal area [m<sup>3</sup>/s/m<sup>2</sup>]  
*f<sub>p</sub>* linear friction factor (energy loss in a porous structure) [-]  
*f<sub>s</sub>* linear friction factor (sponge layer) [-]  
*e<sub>f</sub>* energy dissipation (bed friction) [-]  
*e<sub>b</sub>* energy dissipation (wave breaking) [-]

Elliptic mild-slope results are introduced to equation (2) and (3) by radiation stresses (Copeland 1985). Time dependant variation of wave parameters, i.e. radiation stresses, are reproduced here by splitting the hydrodynamic time scale into several parts.

### 2.2.3 Sediment transport module

Sediment fractions with a grain size diameter less than 60µm are considered as cohesive sediment. Fractions with a diameter larger then 60µm will be considered as non-cohesive material. To describe sediment concentration at a given time and location for both materials, the so-called advection-dispersion equation for the two dimensional case has to be solved:

$$\frac{\partial \bar{c}}{\partial t} + u \frac{\partial \bar{c}}{\partial x} + v \frac{\partial \bar{c}}{\partial y} = \frac{1}{h} \frac{\partial}{\partial x} \left( h D_x \frac{\partial \bar{c}}{\partial x} \right) + \frac{1}{h} \frac{\partial}{\partial y} \left( h D_y \frac{\partial \bar{c}}{\partial y} \right) + Q_L C_L \frac{1}{h} - S \quad (7)$$

- where:  
 $\bar{c}$  depth averaged concentration [g/m<sup>3</sup>]  
*u, v* depth averaged flow velocities [m/s]  
*D<sub>x</sub>, D<sub>y</sub>* dispersion coefficients [m<sup>2</sup>/s]  
*h* water depth [m]  
*S* deposition/erosion term [g/m<sup>3</sup>/s]  
*Q<sub>L</sub>* disch. per unit horiz. area [m<sup>3</sup>/s/m<sup>2</sup>]  
*C<sub>L</sub>* concentration of discharge [g/m<sup>3</sup>]

The characteristics of mud and sand transport used to describe deposition and erosion are realized by different approaches for the deposition/erosion term *S* described in detail by van Rijn (1984) and Englund & Fredsoe (1976).

## 3 PARAMETER STUDIES

### 3.1 Parameter study for mean conditions

The numerical parameter study included the parameters described in Table 1. Parameters used for the 48 test cases in the hydrodynamic, elliptic mild-slope and sediment transport modules are shown in Table 2, 3 and 4.

Table 1. Variation of input parameters (48 test cases).

tidal opening: 25m, 35m, 40m, 50m, 70m, 90m
ditches: yes / no (see also Table 2)
earth embankment: yes / no (see also Table 2)
number of fields: 1 or 2

Table 2: Parameters for the hydrodynamic model (see also Fig. 2 and Fig. 3).

tide: MThw (developed from tidal curve in the project area „Ockholm“)
bathymetry: slope 1:800 for the whole model area
grid spacing: Δx = Δy = 2.00 m
height of brushwood fences: MThw, to prevent overtopping of brushwood fences
porosity of brushwood fence: 20 %
field dimensions: width = 200 m, length = 200 m
number of fields: 1 or 2
main ditch: width = 3.00 m* depth = 0.40 m
cross ditch and 15m ditch: width = 2.00 m depth = 0.40 m
ditches: width = 2.50 m,** depth = 0.40 m distance = 10 m
flood/dry depth: flood depth = 0.25 m dry depth = 0.10 m
ditch adjacent to fences: width = 2.50 m depth = 0.25 m
distance to brushwood fence: 3.00 m*
geometry of earth embankment: height = 0.60 m slope 1:3.33

\*modeled with two grid nodes

\*\* modeled with one grid node

Table 3. Parameters used for the elliptic mild-slope wave model

wave direction perpendicular to the coast
wind effects are ignored
grid spacing: Δx = Δy = 0.50 m
wave period: 3 s
partial reflection coeff. at brushwood fences: 1.5
accuracy: 1.7 %
water depth/wave height: 0.40m/0.08m, 0.50m/0.10m, 0.60m/0.15m, 0.80m/0.20m, 0.90m/0.23m, 1.25m/0.13m

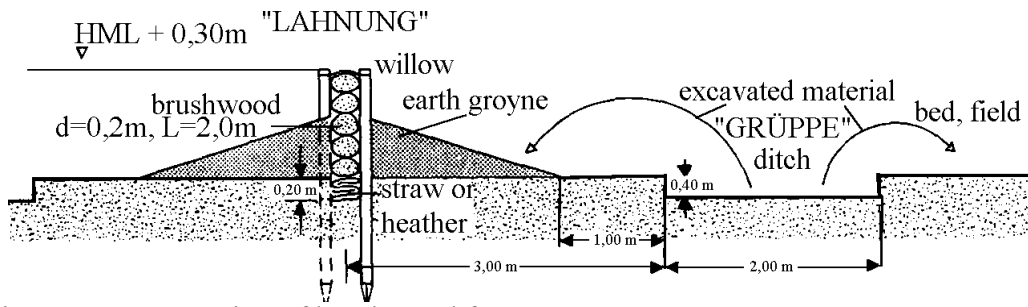


Figure 2: Construction of brushwood fences.

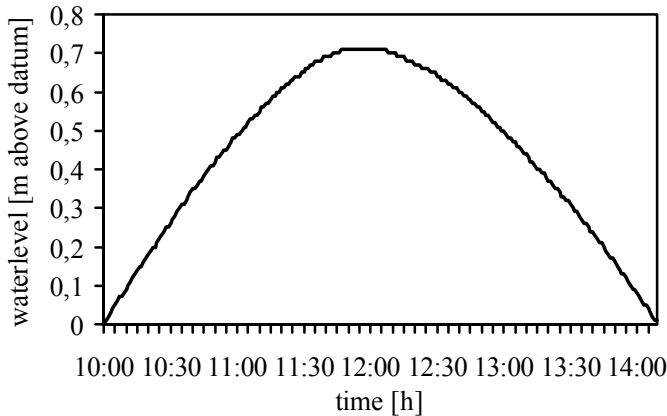


Figure 3: Partial model tide for parameter study under mean conditions.

Table 4. Parameters used for the sediment transport model.

frac. 1 (1 $\mu$ m)	frac. 2 (6 $\mu$ m)	frac. 3 (10 $\mu$ m)
critical velocity for deposition [m/s]		
0.05	0.06	0.07
critical velocity for erosion [m/s]		
0.30	0.30	0.30
mean settling velocity [m/s]		
$7.3 \cdot 10^{-6}$	$2.6 \cdot 10^{-5}$	$7.3 \cdot 10^{-5}$
relative height of centroid [-]		
0.3	0.3	0.3
erosion coefficient [kg/s/m <sup>2</sup> ]		
0.0005	0.0005	0.0005
initial bed composition [-]		
6	13	1
dispersion coefficient in x-direction [m <sup>2</sup> /s]		
0.1	0.1	0.1
dispersion coefficient in y-direction [m <sup>2</sup> /s]		
0.1	0.1	0.1
initial concentration at boundary [g/m <sup>3</sup> ]		
105.0	227.5	17.5

A Manning factor number of  $1.25 \text{ m}^{1/3}/\text{s}$  for the brushwood fence was determined from physical experiments, and for the rest of the model area values were obtained by calibration of the numeric model using data from the test site „Ockholm“. „Sponge layers“ were incorporated at the system boundaries to prevent wave reflection. The results of the Elliptic Mild-Slope Module were transferred to the hydrodynamic module for the tidal phase from which effects of waves on the hydrodynamic behavior of the system (i.e. velocity field) are calculated.

### 3.2 Parameter study for extreme events

For the numerical parameter study of extreme events, two model tides were selected from field data (available data for a period from 1994 to 1995 in the test area „Ockholm“, selected events in jan. and feb. 1995, Fig. 4 and Fig. 5) and transferred to datum.

Wave parameters (Tab. 5) were also selected for the according periods from field data. The friction parameter for modeling the permeable behavior of brushwood fences was calculated with the „reflect“ subroutine. Transmission coefficients  $K_T$  [-] were selected from experiments as parameter input for this algorithm.

All other parameters (like bathymetry, bottom roughness, drainage system) were taken from the parameter set for mean conditions.

The influence of extreme events (case 1 and 2 for tide 3 and case 3 and 4 for tide 47, Tab. 5) were calculated for the first 24 test cases described in Chpt. 3.1.

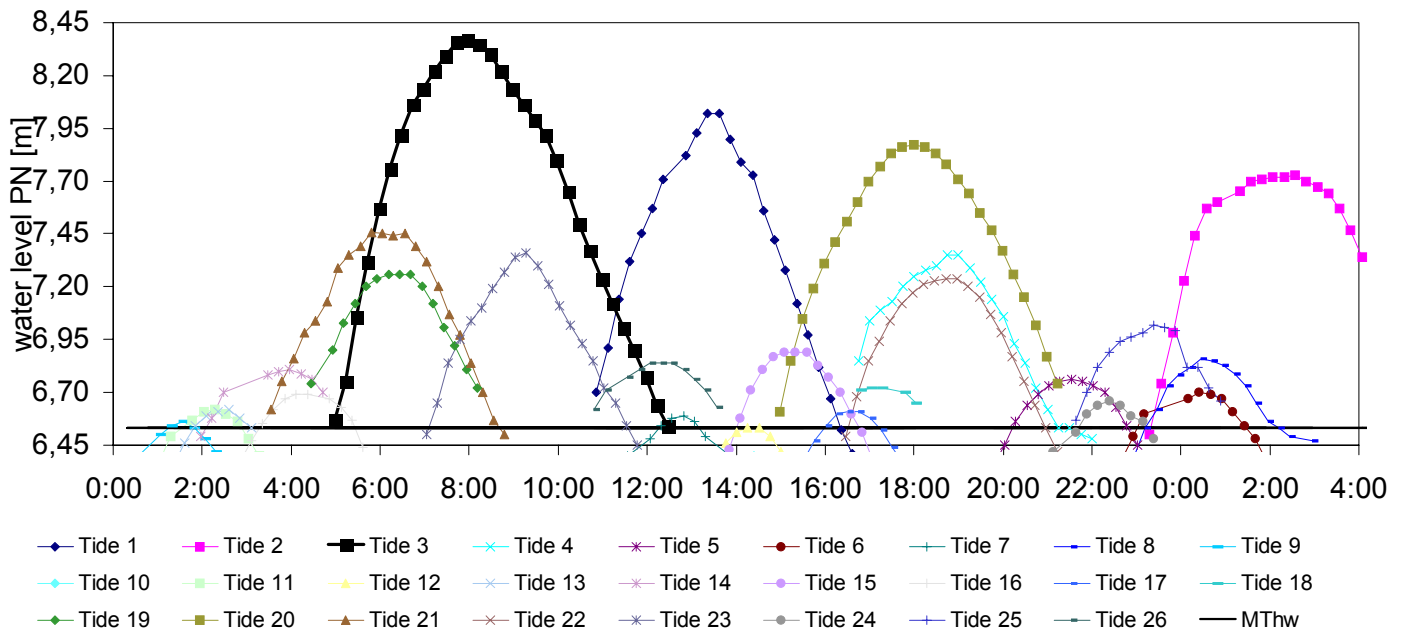


Figure 4. Field data in the test area „Ockholm“ to identify extreme events (jan. 1995, tide 3 selected).

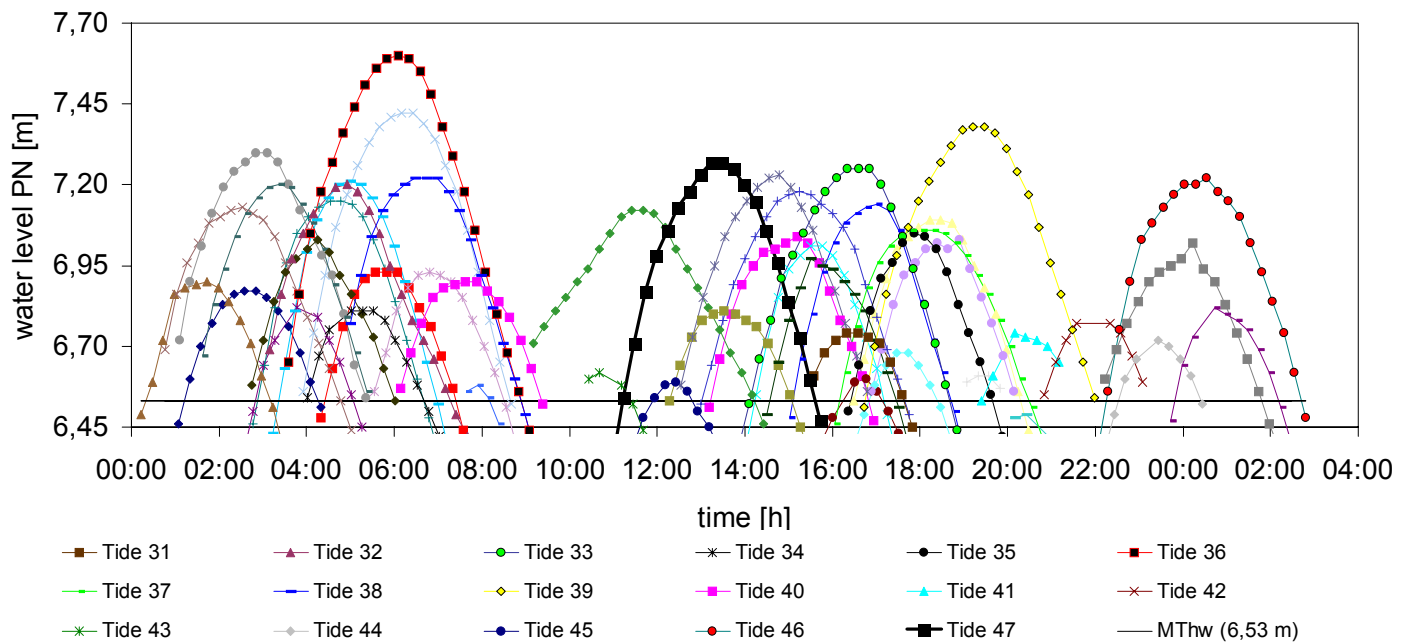


Figure 5. Field data in the project area „Ockholm“ to identify extreme events (feb. 1995, tide 47 selected).

Table 5. Selected wave parameters from field data and calculated friction parameters for EMS-calculations.

Tide 3	case 1 (1./3. tidal phase)		case 1 (2. tidal phase)		case 2 (1./3. tidal phase)		case 2 (2. tidal phase)	
	(a)	(b)	(a)	(b)	(a)	(b)	(a)	(b)
Hs [m]	0.22	0.22	0.22	0.22	0.31	0.31	0.31	0.31
Tp [s]	6.53	6.53	6.53	6.53	3.45	3.45	3.45	3.45
$K_T$ [-]	0.99	0.87	0.99	0.87	0.92	0.85	0.92	0.85
friction [-]	0.20	0.70	0.20	0.70	0.20	0.70	0.20	0.70
Tide 47	Case 3 (1./3. tidal phase)		Case 3 (2. tidal phase)		Case 4 (1./3. tidal phase)		Case 2 (2. tidal phase)	
	(a)	(b)	(a)	(b)	(a)	(b)	(a)	(b)
Hs [m]	0.12	0.12	0.12	0.12	0.18	0.18	0.18	0.18
Tp [s]	4.02	4.02	4.02	4.02	3.08	3.08	3.08	3.08
$K_T$ [-]	0.95	0.89	0.95	0.89	0.91	0.88	0.91	0.88
friction [-]	0.20	0.30	0.20	0.30	0.20	0.30	0.20	0.30

(a) test cases without earth embankment; (b) test cases with earth embankment

## 4 RESULTS

### 4.1 System behavior under mean conditions

The hydrodynamic simulations show a variation in maximum flow velocities in the main direction (perpendicular to the coast) in the middle of the tidal opening. Results show only slight differences between one- and two-field cases, and are too small to affect overall system behavior. The influence of earth embankments can be neglected for tidal opening larger than 70m. Only in the middle of the fields, changes in tidal opening width lead to significant variations in wave heights. Under certain conditions, reflection and diffraction effects can increase wave heights in the field to values higher than outside the field. Results show satisfactory agreement with field data (Matheja et al., 1997).

Sedimentation results show the influence of tidal opening width (here only presented for m\_01 and m\_06 in Fig. 6 and Fig. 7), earth embankment and ditches (Tab. 6).

Table 6. Sedimentation [kg] after one model tide under mean conditions.

test case	tidal opening [m]	„land field“	„sea field“
one field, no ditches, no earth embankment			
m_01	25	2551	
m_06	90	2517	
two fields, no ditches, no earth embankment			
m_07	25	2149	2131
m_12	90	1990	2089
one field, no ditches, earth embankment			
m_13	25	2087	
m_18	90	1739	
two fields, no ditches, earth embankment			
m_19	25	1893	1794
m_24	90	1621	1681
one field, ditches, no earth embankment			
m_25	25	2435	
m_30	90	2169	
two fields, ditches, no earth embankment			
m_31	25	2278	2999
m_36	90	1851	2463
one field, ditches, earth embankment			
m_37	25	3336	
m_42	90	3138	
two fields, ditches, earth embankment			
m_43	25	2475	2499
m_48	90	2185	2271

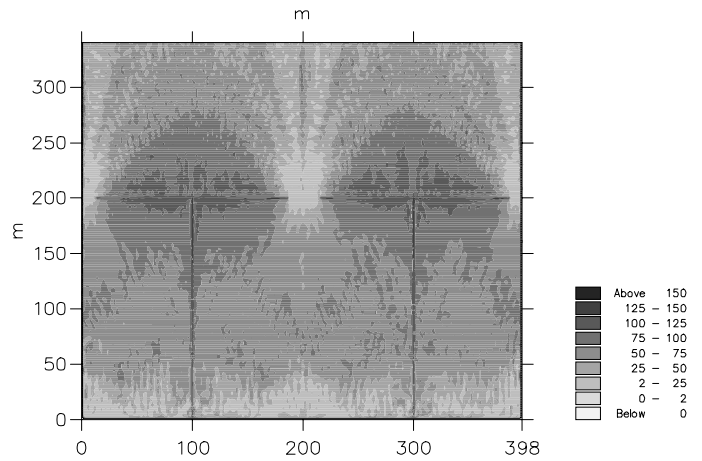


Figure 6. Sedimentation/Erosion after one model tide [g/m<sup>2</sup>] (test case m\_01: one field, no ditches, no earth embankment, tidal opening = 25 m, levels: Below 0; 0 - 2; 2 - 25; 25 - 50; 50 - 75; 75 - 100; 100 - 125; 125 - 150; Above 150; from light to dark)

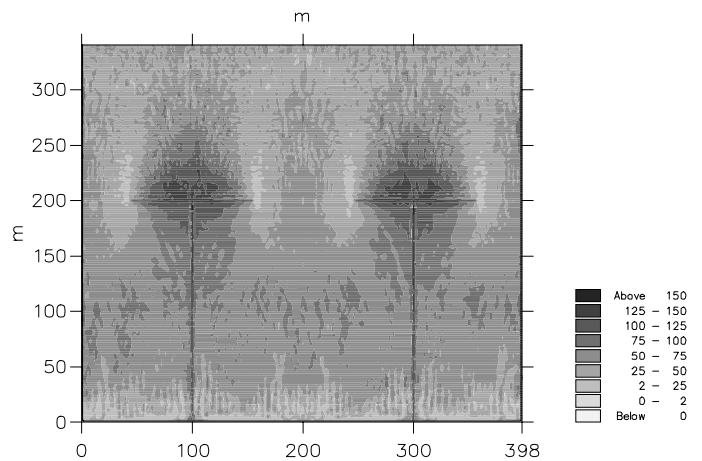


Figure 7. Sedimentation/Erosion after one model tide [g/m<sup>2</sup>] (test case m\_06: one field, no ditches, no earth embankment, tidal opening = 90 m, levels: Below 0; 0 - 2; 2 - 25; 25 - 50; 50 - 75; 75 - 100; 100 - 125; 125 - 150; Above 150; from light to dark)

With larger tidal openings, there is a marked decrease in sedimentation in field corners. In front of fence interchanges points sedimentation rates increase as a result of calmer currents in these areas. This is seen in two field-cases.

With earth embankment, fences act as impermeable walls, so no sediment transport occurs across them (assuming no overtopping). In one-field cases with ditches, no influence is visible. Sedimentation in front of fence interchanges points increases for all test cases. In two-field cases, areas with lower sedimentation in the middle of the „sea-field“ become larger.

Besides ditches sedimentation increases significantly. Tidal currents, entering the field along the main ditch, prevent sedimentation processes in the first 70 m of this ditch and in a semicircle of 25 m diameter from the center of the tidal opening. For two-field cases, ditches lead to more sedimentation

in corners of the „sea field“. Sedimentation distribution in the „land field“ is much more regular, than for cases without ditches. Ditches act as a very efficient sediment trap.

Two-field cases show a significant decrease of sedimentation in the tidal opening of „land fields“ and in a semicircle of about 35 m diameter extending from the center of the opening.

Overall sedimentation after one model tide (linear behavior between the described cases in Tab. 5 for varied tidal opening width) decreases as the width of tidal opening increases. It is found that systems with earth embankment hinder sedimentation, i.e. suppress sediment transport across brushwood fences. Ditches in systems with earth embankment give higher sedimentation rates.

4.2 System behavior during extreme events

Results show the effect of different wave- and tide-induced currents for extreme events on mud and sand transport, and thus sedimentation and erosion (Tab. 7).

Increase of sedimentation is considerable (except case m\_24, case 4).

With larger tidal openings sedimentation decreases. In all test cases the eroded areas in the surrounding of tidal opening become smaller as openings increase for case 1 and 2 (Tab. 7).

In test cases 3 and 4 eroded areas are not visible in all test cases.

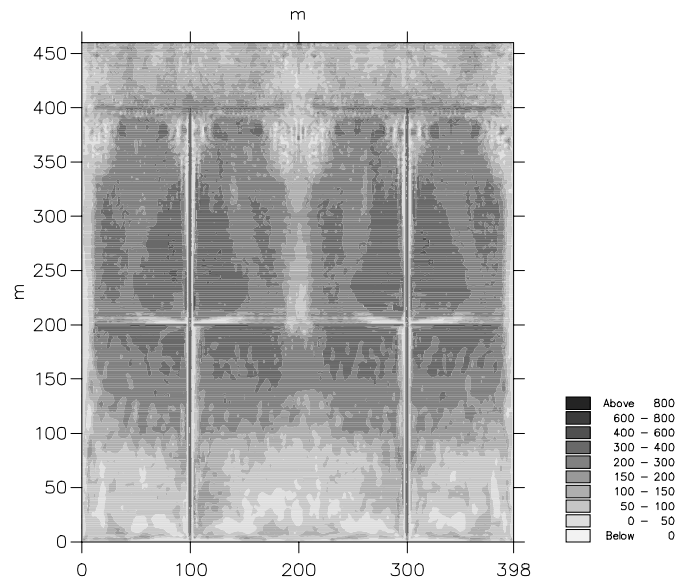


Figure 8. Sedimentation/Erosion after one model tide [g/m<sup>2</sup>] (test case m\_07, case 2: two fields, no ditches, no earth embankment, tidal opening = 25 m, levels: Below 0; 0 - 50; 50 - 100; 100 - 150; 150 - 200; 200 - 300; 300 - 400; 400 - 600; Above 600; from light to dark)

With earth embankment, fences act as impermeable walls near the bottom, so sediment transport

across fences is limited to higher water levels. Overall sedimentation decreases in all these test cases (up to approximately 60%). Maximum decrease is observed for larger tidal opening.

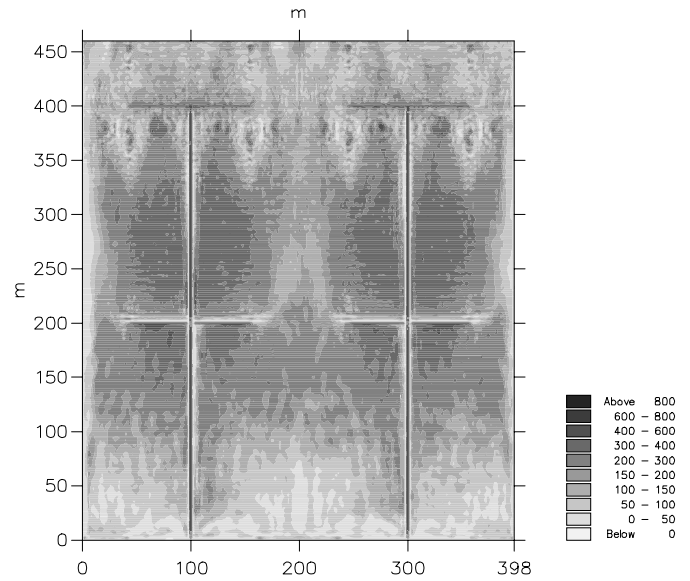


Figure 9. Sedimentation/Erosion after one model tide [g/m<sup>2</sup>] (test case m\_12, case 2: two fields, no ditches, no earth embankment, tidal opening = 90 m, levels: see Fig. 8)

Table 8. Development of water volume over one model tide in „land fields“.

	mean tide	tide 3	tide 47
start / final vol. [m <sup>3</sup> ]	0	22800	14000
max. vol. [m <sup>3</sup> ]	32400	94800	50800

In one-field case sedimentation in front of fence crossing points increases for all test cases. For two-field cases sedimentation in these areas disappear.

In two-field cases, areas with lower sedimentation in the middle of the „sea-field“ become larger (Fig. 8 and Fig. 9).

Two-field cases with earth embankment show a significant decrease (50 - 60 %) of sedimentation in the „sea field“. Without earth embankment sedimentation decreases (30 %) in „land fields“.

From comparison of case 1/2 and 3/4 follows a decrease of sedimentation for higher waves. The effect of waves becomes evident in the „land fields“ of two-field cases.

In all cases the influence of wave characteristics stands behind the influence of flooding period (7.5 h for tide 3, 4,45 h for tide 47), maximal flooding depth (1.8 m for tide 3, 0.92 m for tide 47), and thus corresponding tidal water volume entering the fields (Tab. 8).

Table 7. Sedimentation [kg] after one model tide under mean conditions and evaluated extreme conditions.

test case	mean conditions		case 1		case 2		case 3		case 4	
	field 1**	field 2***	field 1**	field 2***	field 1**	field 2***	field 1**	field 2***	field 1**	field 2***
one field, no ditches, no earth embankment										
m_01	2551		11889		10550		7246		6588	
m_06	2517		11418		9586		7021		6388	
two fields, no ditches, no earth embankment										
m_07	2149	2131	10850	11303	6733	9420	6590	6875	4715	5506
m_12	1990	2089	10080	10292	6480	8680	6380	6636	4727	5429
one field, no ditches, earth embankment										
m_13	2087		8835		7148		5221		2883	
m_18	1739		5794		4375		4376		2233	
two fields, no ditches, earth embankment										
m_19	1893	1794	9596	5829	4418	1834	3852	1866	*	*
m_24	1621	1681	6022	5120	2877	2293	2557	2019	1662	1055

\* test case not calculated, \*\* field 1 = „land field“, \*\*\* field 2 = „sea field“

## 5 CONCLUSIONS

The parameter studies are based on numerical models, restricted due to idealized conditions (like tides, wave characteristics, wave attack perpendicular to the coast, fractions). They are also based on field data and experimental studies (physical models), which ensure transferability and applicability of the applied approach.

System behavior under mean conditions show, that efficiency of this protection system strongly depends on system geometry (height of the fences, width of tidal opening and field dimensions), permeability of brushwood fences (applied material and earth embankment) and dimensions of the drainage system (number of ditches, incorporation of main ditches).

It also shows, that the influence of extreme events like wave attack, tidal currents, and thus failure of brushwood fences is uncritical for investigated scenarios.

Sedimentation under extreme conditions increases significantly, due to higher tidal water exchange and longer flooding period. Wave attack and currents can not compensate this phenomena for tested parameter sets and boundary conditions.

Prediction of foreland growth enables evaluation of earlier wave breaking and thus higher energy losses in forelands during severe storm events. Results are applicable to other coastal regions, lagoons and estuaries, where sedimentation fields are used as sedimentation traps for land reclamation and foreland development.

Embedding the analyzed local processes in a regional context to ensure sustainable foreland management and development for longer coastlines and numerical simulation of long-term behavior will be research topics in the future.

## REFERENCES

- Berkhoff, J.C.W. 1972. Computation of combined refraction-diffraction. Proc. 13<sup>th</sup> Coastal Eng. Conf., Vancouver, 1972: Vol.1, 471-490. New York: ASCE.
- Copeland, G.J.M. 1985. Practical radiation stress calculations connected with equations of wave propagation. Coastal Engineering, Vol. 9, 195-219.
- Engelund, F. & J. Fredsoe 1976. A sediment transport model for straight alluvial channels. Nordic Hydrology, Vol. 7, 293-306.
- Madsen, P.A. & J. Larsen 1987. An efficient finite-difference approach to the mild-slope equation. Coastal Engineering, Vol. 11, 329-351.
- Matheja, A.; von Lieberman, N. & C. Zimmermann 1997. Land reclamation and coastal protection in shallow tidal waters - A numerical case study in the German Wadden sea area. In: Proc. of the 1<sup>st</sup> International Conf. Port, Coast, Environment, Varna, 30 June - 4 July 1997: Vol. 1, 62-72.
- Richtmeyer, R.D. & K.W. Morton 1967. Difference Methods for Initial Value Problems. 2<sup>nd</sup> Ed., New York: Interscience.
- van Rijn, L.C. 1984. Sediment Transport, Part I: Bed Load Transport, Part II: Suspended Load Transport. Journal of Hydraulic Engineering, 110(10).
- Warren, I.R.; Larsen, J. & P.A. Madsen 1985. Application of short wave numerical models to harbor design and future development of the model. Int. Conf. on Numerical and Hydraulic Modeling of Ports and Harbors, Birmingham, April 1985.